SCIENCE CHINA
Technological Sciences

• Article •

August 2014 Vol.57 No.8: 1616–1625
doi: 10.1007/s11431-014-5551-z

Investigation on mechanism of polymer filling in high-aspect-ratio trenches for through-silicon-via (TSV) application

DING YingTao, YAN YangYang, CHEN QianWen, WANG ShiWei, CHEN Xiu & CHEN YueYang*

School of Information and Electronics, Beijing Institute of Technology, Beijing100081, China

Received September 25, 2013; accepted January 15, 2014

Vacuum-assisted spin-coating is an effective polymer filling technology for sidewall insulating of through-silicon-via (TSV). This paper investigated the flow mechanism of the vacuum-assisted polymer filling process based on experiments and numerical simulation, and studied the effect of vacuum pressure, viscosity of polymer and aspect-ratio of trench on the filling performance. A 2D axisymmetric model, consisting of polymer partially filled into the trench and void at the bottom of trench, was developed for the computational fluid dynamics (CFD) simulation. The simulation results indicate that the vacuum-assisted polymer filling process goes through four stages, including bubble formation, bubble burst, air elimination and polymer re-filling. Moreover, the simulation results suggest that the pressure significantly affects the bubble formation and the polymer re-filling procedure, and the polymer viscosity and the trench aspect-ratio influence the duration of air elimination.

through-silicon-via (TSV), vacuum process, polymer filling, computational fluid dynamics (CFD)

Citation: Ding Y T, Yan Y Y, Chen Q W, et al. Investigation on mechanism of polymer filling in high-aspect-ratio trenches for through-silicon-via (TSV) application. Sci China Tech Sci, 2014, 57: 1616–1625, doi: 10.1007/s11431-014-5551-z

1 Introduction

Through-silicon-via (TSV), which passes through the substrate to vertically stack devices, has great potential for widespread use in advanced microelectronic systems with high speed, high density, small size and multifunction [1–4]. TSV can greatly reduce the global interconnect length byreplacing the long global metal interconnect with short TSV structure, leading to the improvement of the electronic performances in speed, bandwidth and power. Additionally, TSV enables the combination of different optimized production technologies, thus becoming one of the key solutions to realize heterogeneous integration. Based on the TSV technology, three-dimensional (3D) integration and silicon interposer approach have been presented and treated as promising technologies for future portable electronic devices [5–8].

However, the sidewall insulating is one of the challenging bottlenecks in the TSV processes, due to the scalloped etch profile produced by the DRIE/Bosch process [9] and the poor step coverage ability of common deposition method [10], such as chemical vapor deposition (CVD). Typically, the thickness of sidewall insulating layer deposited by CVD is higher at the top, and would be highly reduced along the depth ofTSV, resulting in poor uniformity [10]. Moreover, the uniformity would further degrade with the increasing of the aspect ratio of TSV. Such non-uniform sidewall insulating cannot ensure the expected insulation properties, such as no leakage, higher breakdown voltage, higher reliability, and no cracking.

To achieve high reliability, polymer insulating TSV [12,13] has been exploited by completely filling trenches to

*Corresponding author (email: chenyuexiang@bit.edu.cn)

form uniform insulation along the depth of TSV [14]. Various polymer filling technologies, including spray [15,16], wetting deposition [17,18], and vacuum lamination [18], as well as conventional spin coating [16,20] and vacuum-assisted spin coating [21] have been investigated to achieve void-free polymer filing of trenches. Among these filling approaches, vacuum-assisted polymer filling has attracted great interest, due to its super filling ability of high-density and high-aspect-ratio trenches (up to 20:1) [22]. However, even though experiments have been carried out to demonstrate the filling ability of the vacuum-assisted polymer filling approach, the filling mechanism and the influence factors of process are not well understood.

This paper investigates the flow mechanism of vacuum-assisted polymer filling in high-aspect-ratio trench using volume of fluid (VOF) modeling with ANSYSsoftware. A two-phase flow model for gas and polymer transport within trench is presented. The volume fraction and mixture velocity are calculated based on computational fluid dynamics (CFD) simulation. Moreover, to guide the perfect realization of void-free filling,the impacts of vacuum pressure, polymer viscosity, and aspect-ratio of trench on the filling performance have been studied.

2 Experiments

To demonstrate the efficiency of vacuum-assisted polymer filling, highaspectratio trenches werefabricated and used as samples to perform the polymer filling experiments. The used polymer is Benzocyclobutene (BCB), due to its attractive properties, such as low dielectric constant (~2.5), excellent chemical resistance, and high thermal stability. The experiments started with trenches etching in 4-inch silicon wafer with a depth around 60 μm using deep reactive ion etching (DRIE) process. Then, the wafer went through the vacuum-assisted filling processes of adhesion promoter (AP 3000, Dow Chemical) and BCB (CYCLOTENE 3000 series/3022-46, Dow Chemical), respectively. During each vacuum-assisted filling process, the executed steps included polymer dispensing, vacuum treating in sealed chamber, high-speed spinning, and soft baking. After that, the wafer was hard cured in a vacuum chamber at 250°C for 60 min to solidify BCB. For comparing analysis, polymer filling with conventional spin coating and partial vacuum treatment were also performed. The detailed steps and corresponding parameters are listed in Table 1. Compared with both the scheme (partial and complete) of the vacuum-assisted processes, the main differences are the chamber pressure, which is 30 kPa for partial vacuum treatment and is only 100 Pa for complete vacuum treatment, respectively.

After polymer filling and hard-curing, the samples were diced for scanning electron microscope (SEM) inspection. The SEM images of polymer filling results are shown in Figures 1–3, corresponding to the samples fabricated by conventional spin-coating, partial vacuum-assisted and complete vacuum-assisted spin-coating, respectively. As can been seen from Figure 1, obvious voids were formed at the bottom of trenches, no matter what the aspect-ratio of the trenches was. The large dishing in Figure 1(a) can be reduced with additional polymer filling, and the slight dishing in Figure 1(b) is due to the second vacuum-assisted polymer filling with BCB. These filling results indicate the poor filling ability of conventional spin-coating method, which only consists of polymer dispersing and high-speed spinning steps. Air inside the trenches would form voids for it was trapped. For the samples fabricated by partial vacuum treatment, as shown in Figure 2, somevoids existed inside the trenches. However, for the samples fabricated by complete vacuum treatment, as shown in Figure 3, the trenches were fully filled with polymer and without any void. The different filling results show that the process parameters play an important role in the filling ability.

3 Simulation

To better understand the flow mechanism and investigate the influence of process parameters on filling performance, a series of cases werecomputed based on the software ANSYS Fluent 14.5.A 2D axisymmetric model was developed, and the detailed geometry dimensions and computation gridswere shown in Figure 4. The void at the bottom of trench was simplified as a rectangle. The polymer was filled

Table 1 Detailed process steps and corresponding parameters

Approach Step	Conventional spin-coating	Partial vacuum-assisted spin-coating	Complete vacuum-assisted pin-coating
Promoter dispensing	5 mL AP3000	10 mL AP3000	10 mL AP3000
Vacuum treating	None	Chamber, 100 Pa, 10 min	Chamber, 100 Pa,10 min
Spin coating	500 r min^{-1}:10 s 3000 r min^{-1}:40 s	500 r min^{-1}:10 s 3000 r min^{-1}:40 s	500 r min^{-1}:10 s 3000 r min^{-1}:40 s
Soft baking	95°C 5 min	95°C 5 min	95°C 5 min
Polymer dispensing	5 mL BCB	10 mL BCB	10 mL BCB
Vacuum treating	None	Chamber,30 kPa, 10 min	Chamber,100 Pa, 10 min
Spin coating	500 r min^{-1} :10 s 3000 r min^{-1} :40 s	500 r min^{-1} :10 s 3000 r min^{-1} :40 s	500 r min^{-1} :10 s 3000 r min^{-1} :40 s
Soft baking	120°C 5 min	120°C 5 min	120°C 5 min
Hard baking	Vacuum chamber curing 250°C 60 min	Vacuum chamber curing 250°C 60 min	Vacuum chamber curing 250°C 60 min

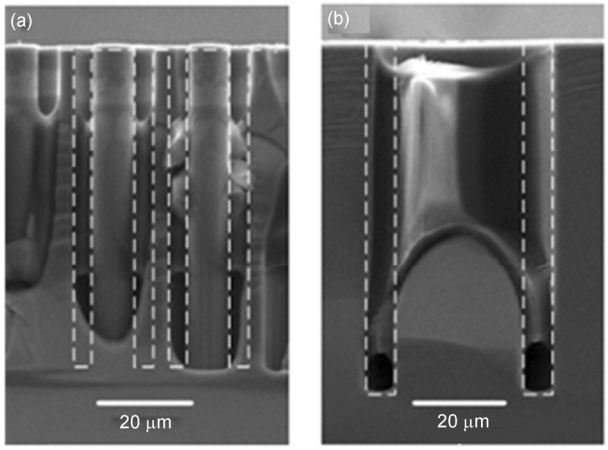

Figure 1 Cross-sectional SEM images of polymer filling in trenches with conventional spin coating. (a) Inner diameter of 10 μm and trench width of 2 μm; (b) inner diameter of 25 μm and trench width of 5 μm.

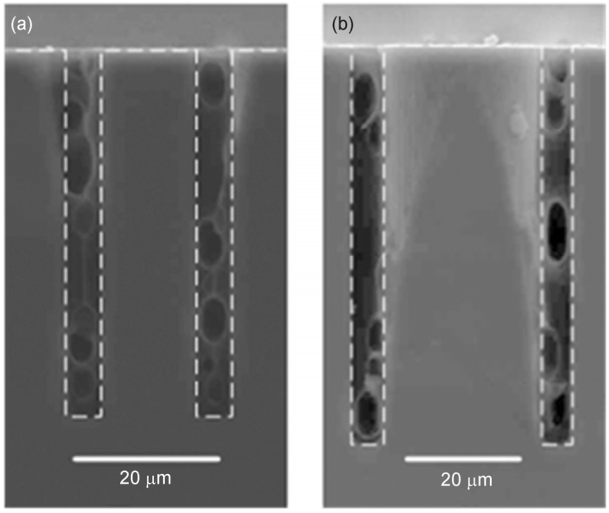

Figure 2 Cross-sectional SEM images of polymer filling in trenches with partial vacuum-assisted spin coating. (a) Inner diameter of 15 μm and trench width of 5μm; (b) inner diameter of 25 μm and trench width of 5 μm.

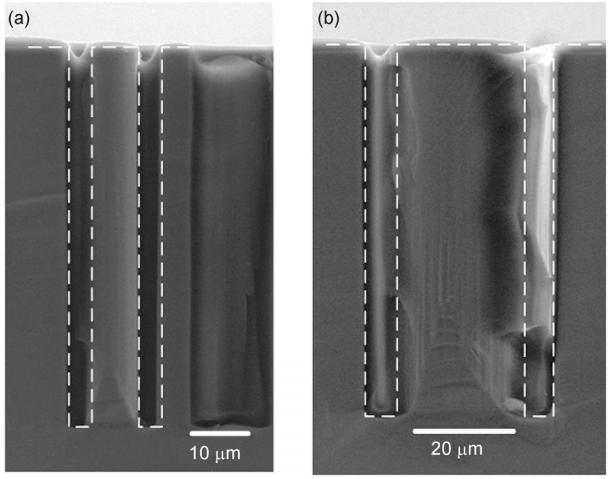

Figure 3 Cross-sectional SEM images of polymer filling in trenches with complete vacuum-assisted spin coating: (a) inner diameter of 10 μm and trench width of 3 μm; (b) inner diameter of 25 μm and trench width of 5 μm.

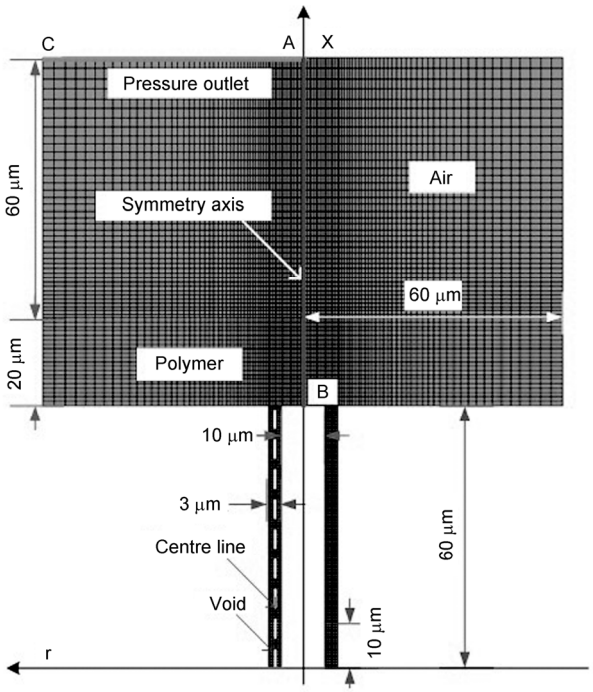

Figure 4 2D axisymmetric model of annular trench partly filled with polymer.

into trench with a 20 μm thickness on the surface. Line AB and line AC represented asymmetry axis and pressure outlet, respectively. The other edges were defined wall. The centre line of annular trenchwasused as the path to record the volume fraction and the velocities. The structure rectangle grids were chosen and the distribution of grids in annular trench field was refined.

3.1 Governing equations

Consider a two-phase flow in a 2D axisymmetric annular trench as shown in Figure 4. The conservation equations of mass are given by

$$\frac{\partial \rho}{\partial t} + \nabla \cdot (\rho \boldsymbol{u}) = S_m, \tag{1}$$

where ρ is fluid density, $\boldsymbol{u}$ is velocity of fluid, and the source S_m is the mass added to the continuous phase from the dispersed secondary phase.

The equations of momentum can be written as [23]

$$\begin{aligned} &\frac{\partial}{\partial t}(\rho \boldsymbol{u}) + \nabla \cdot (\rho \boldsymbol{u}\boldsymbol{u}) \\ &= -\nabla p + \mu \left[\left(\nabla \boldsymbol{u} + \nabla \boldsymbol{u}^T - \frac{2}{3} \nabla \cdot \boldsymbol{u} \boldsymbol{I} \right) \right] + \rho \boldsymbol{g} + \boldsymbol{F}, \end{aligned} \tag{2}$$

Where p is the static pressure, μ is dynamic viscosity, and $\rho \boldsymbol{g}$, $\boldsymbol{F}$ are the gravitational body force and external force respectively. Due to a small role in microflow, the gravity is

usually neglected. When considering 2D axisymmetric geometries, the converted momentum conservation equation in axial and radial directions can be given by

$$\begin{aligned}&\frac{\partial}{\partial t}(\rho u_x)+\frac{1}{r}\frac{\partial}{\partial x}(r\rho u_x u_x)+\frac{1}{r}\frac{\partial}{\partial r}(r\rho u_r u_x)\\&=-\frac{\partial p}{\partial x}+\frac{1}{r}\frac{\partial}{\partial x}\left[r\mu\left(2\frac{\partial u_x}{\partial x}-\frac{2}{3}\left(\nabla\cdot\vec{u}\right)\right)\right]\\&+\frac{1}{r}\frac{\partial}{\partial r}\left[r\mu\left(\frac{\partial u_x}{\partial r}+\frac{\partial u_r}{\partial x}\right)\right]+F_x,\end{aligned}\tag{3}$$

and

$$\begin{aligned}&\frac{\partial}{\partial t}(\rho u_r)+\frac{1}{r}\frac{\partial}{\partial x}(r\rho u_x u_r)+\frac{1}{r}\frac{\partial}{\partial r}(r\rho u_r u_r)\\&=-\frac{\partial p}{\partial r}+\frac{1}{r}\frac{\partial}{\partial r}\left[r\mu\left(2\frac{\partial u_r}{\partial r}-\frac{2}{3}\left(\nabla\cdot\vec{u}\right)\right)\right]\\&+\frac{1}{r}\frac{\partial}{\partial x}\left[r\mu\left(\frac{\partial u_r}{\partial x}+\frac{\partial u_x}{\partial r}\right)\right]\\&-2\mu\frac{u_r}{r^2}+\frac{2}{3}\frac{\mu}{r}\left(\nabla\cdot\vec{u}\right)+\rho\frac{u_z^{\,2}}{r}+F_r,\end{aligned}\tag{4}$$

where r is the radial direction, x is the axial direction, u_z is the swirl velocity.

The continuum surface force (CSF) put forward by Brackbill et al. [24] has been used to deal with the surface tension. Expressed as a volume force using the divergence theorem, the force at the surface is the source term which is added to the momentum equation. For two-phase flow, it has the following form

$$F_{vol}=\sigma\frac{\rho\kappa_2\nabla\alpha_2}{0.5\left(\rho_1+\rho_2\right)},\tag{5}$$

Where σ is surface tension coefficient, α presents the volume fraction, subscripts 1 and 2 represent primary phase and secondary phase respectively, κ_2 is the divergence of the unit normal $\hat{n}$ and $\kappa_2=\nabla\cdot\hat{n}$, $\hat{n}=n/|n|$, $n=\nabla\alpha_2$.

3.2 Boundary and initial conditions

Apressure outlet boundary is specified at the exit and a no-slip condition is applied at the wall. The constant temperature (300 K) is assumed in all the zones. A cylinder bubble of 10 μm in length is placed at the bottom of the trench and the remaining trench is filled with the polymer. An outlet pressure function plotted in Figure 5 is used to initialize the flow. The pressure decreases from 100 to 1 kPa at the beginning. Then the pressure of 1 kPa is kept for 600 s. Finally, it is pumped up to 100 kPa. Air (typically ideal gas) is designated as the primary phase, and polymer (shown in Table 2) is defined as the secondary phase.

Table 2 Properties of CYCLOTENE 3000 series [25]

Properties	3022-35	3022-46	3022-57
Resin content (%)	35	46	57
Density (kg/m^3 at 5°C)	930	950	970
Viscosity (cSt at 25°C)	14	52	259

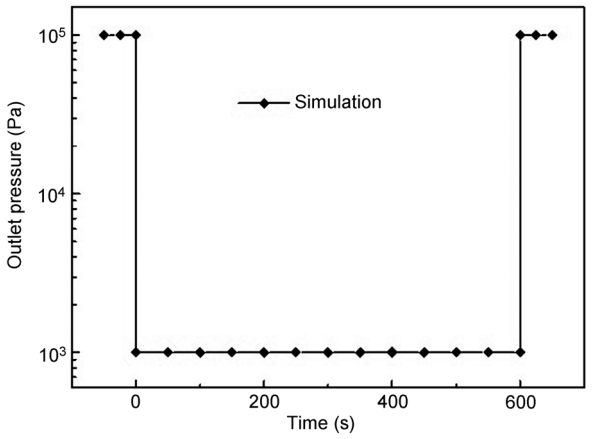

Figure 5 Relationship between outlet pressure and time.

3.3 Volume of fluid (VOF) method

The working media of vacuum process are air (gas) and polymer (liquid). So volume of fluid (VOF) [26] method is considered to describe the two-phase flow issue. It is known for its capacity for interface tracking of immiscible fluid by introducing a volume fraction function of phase α. Taking this case as an example, α presents the volume fraction of air in a unit cell, then $1-\alpha$ is volume fraction of polymer. There are three conditions given as follows

α=1: The cell is full of air;

α=0: The cell is empty of air, in other words, is full of polymer;

0<α<1: The cell contains both air and polymer.

The density and viscosity of the cell can be written as

$$\rho=\alpha\rho_{\text{air}}+(1-\alpha)\rho_{\text{polymer}},\tag{6}$$

$$\mu=\alpha\mu_{\text{air}}+(1-\alpha)\mu_{\text{polymer}}.\tag{7}$$

For realizing the tracking of the interface between the two phases, the continuity equation for the volume fraction is written as

$$\frac{1}{\rho_2}\left[\frac{\partial}{\partial t}\left(\alpha_2\rho_2\right)+\nabla\left(\alpha_2\rho_2\boldsymbol{u}_2\right)\right]=\dot{m}_{12}-\dot{m}_{21},\tag{8}$$

where subscripts 1 and 2 represent primary phase and secondary phase respectively, $\dot{m}_{12}$ is the mass transfer from phase 1 to phase 2 and $\dot{m}_{21}$ is the adverse one.

4 Results

The flow mechanism of the vacuum-assisted polymer

filling would be discussed in this section. And, the filling performance would be studied with variations of vacuum pressure (1, 10, and 50 kPa), polymer properties (shown in Table 2) and trench width (2, 3 and 5 μm).

4.1 Flow mechanism of vacuum-assisted polymer filling process

The simulation results illustrate that the whole vacuum-assisted polymer filling process goes through four stages, including sharply bubble formation, obvious bubble burst, successive air elimination and effective polymer re-filling, as shown from Figures 6(a) to (d), respectively. From Figure 6(a), it can be seen that initial void sharply expands, and BCB is squeezed out of the trench, further leading to obvious bubble formation. It should be pointed out that the obvious bubble is formed within an extremely short duration (24 ms), and has a size as large as 50 μm. Such large bubble wasalso obviously observed during the experiments. With further increasing of the vacuum treatment duration, as shown in Figure 6(b), the film thickness of bubble becomes thinner, and the bubble finally bursts after vacuum treatment for 12 s. At this moment, the trench is almost occupied by air, and only tiny polymer exists on the sidewall of the trench. Then, as shown in Figure 6(c), the air successively escapes from the trench, and the polymer starts to refill the trench. This stage is time consuming, and could be maintained up to 600 s. After that, when the outlet pressure is set back to atmospheric pressure, BCB is quickly compelled back to trench and the volume of voids is reduced exponentially, as shown in Figure 6(d). Finally, at 650 s the trench is almost fully filled with BCB, only consisting of tiny air-polymer mixture, which is shown in Figure 6(d).

To clearly understand the air elimination procedure and

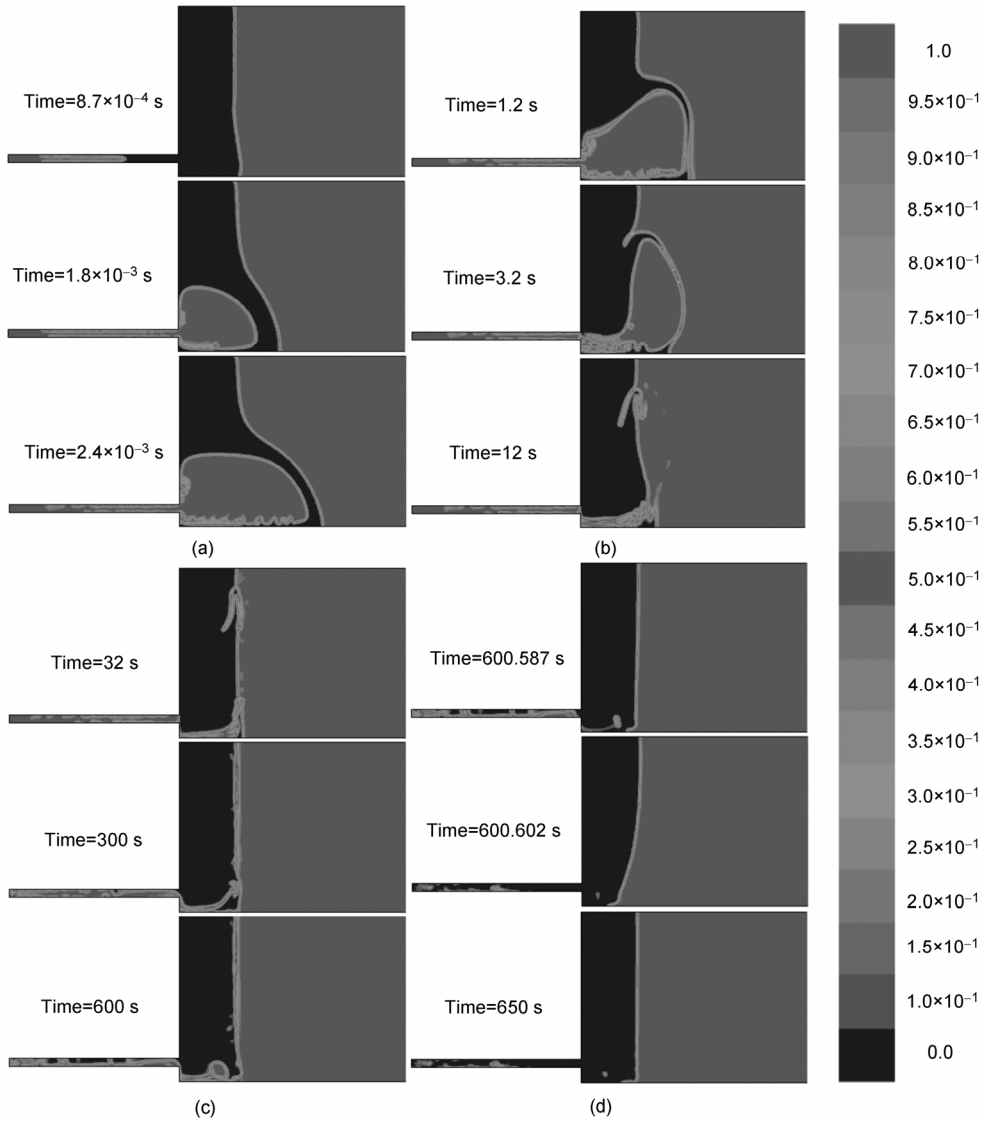

Figure 6 Contour of volume fraction within the vacuum-assisted polymer filling process, including. (a) Bubble formation; (b) bubble burst; (c) air elimination; and (d) polymer re-filling.

investigate the mechanism of the vacuum-assisted polymer filling, the corresponding mixture velocities along the centre line of annular trench are plotted in Figure 7. As plotted in Figure 7(a), during the bubble formation, the velocity at the entrance of trench is less than 0.05 m/s at the beginning,then significantly increases to 0.6 m/s at the outlet after1.8 ms, and decreases to zero with the further increasing of duration. Such sharp velocity variation is mainly due to the interaction of pressure difference and viscous force. Just as the pressure shown in Figure 8 and the volume fraction shown in Figure 9, at the beginning (0.87 ms), even though large driving force is formed by larger pressure difference (circle curve in Figure 8), the significant viscous force due to BCB constrained within the trench (circle curve in Figure 9) would greatly limit the velocity. While BCB is squeezed out of the trench at 1.8 ms (triangle curve in Figure 9), the viscous force is highly reduced, and large velocity can be achieved by the pressure difference. Subsequently, the pressure difference rapidly decreases, and a pressure balance between inside and outside of the trench is achievedat 24 ms (inverted triangle curve in Figure 8), resulting in the low velocity. Figures 7(b) and (c) show that the velocities at the bubble burst and air elimination stage are low, in the range of μm/s, which are three-orders lower than that at the bubble formation stage. It is due to the lack of driving force generated by pressure difference and the limitation of inevitable viscous force [27]. It will take sufficient duration to perform the air elimination, which will directly affect the filling performance. If the trapped air cannot completely escape from the trench, void will exist after the polymer re-filling process. Figure 7(d) shows that velocity of 0.08 m/s can be achieved by setting the outlet pressure back to atmosphere pressure (100 kPa), due to driving force generated by pressure difference. Even though the pressure difference only exists in the short duration, which is less than 5 ms, it is powerful to effectively push the polymer to refill the trench.

4.2 Effect of pressure on filling performance

Figures 10 and 11 show the effect of outlet pressure on the contour and centerline distribution of volume fraction at two different moments. One moment is at 24 ms when voids stop expanding, the other one is at 650 s when polymers start re-filling.

From Figure 10(a), it is seen that void expandsmuch faster at lower outlet pressure, leading to obvious bubble formation for 1 and 10 kPa. This can be better understood from Figure 11(a). For the case of 1 kPa (square curve) and 10 kPa (circle curve), the volume fraction of BCB in trench decreases almost to zero, namely, the polymer has been almost completely expelled from the trench. But in the case of 50 kPa (triangle curve), it can be seen that the void only expands double compared with initial volume, and the polymer cannot be squeezed out of the trench. Even by further increasing the duration, obvious bubble cannot be for-

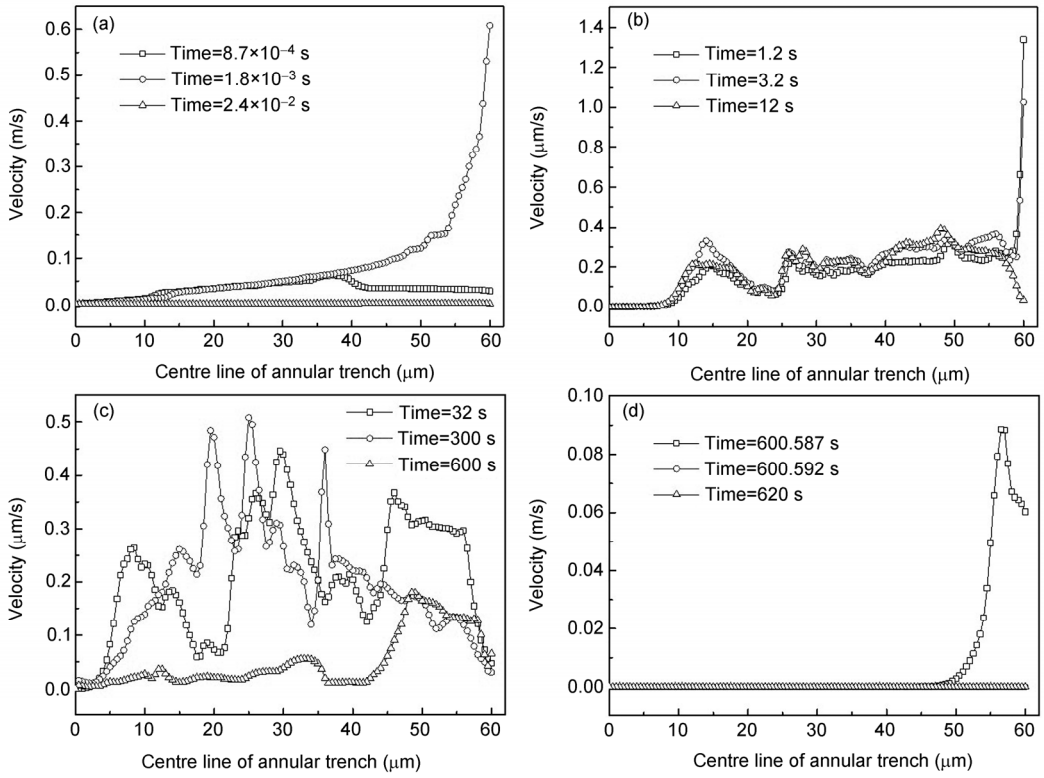

Figure 7 Mixturevelocity along the centre line of annular trench within different stages. (a) Bubble formation; (b) bubble burst; (c) air elimination; and (d) polymer re-filling.

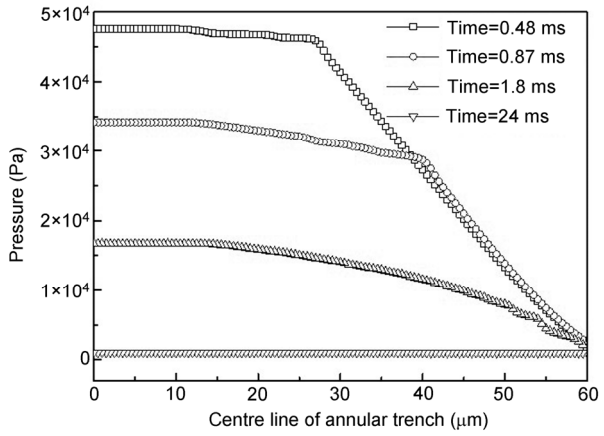

Figure 8 Pressure along the centre line of annular trench at different times.

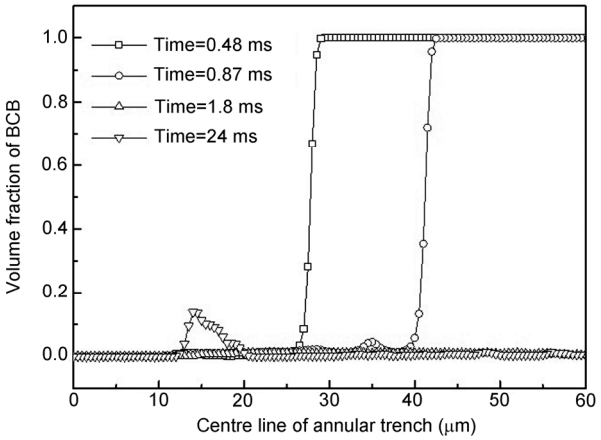

Figure 9 Volume fraction of BCB along the centre line of annular trench at different times.

med, limiting the air elimination.

After BCB re-filling (Figure 10(b)), there is a better filling performance for lower outlet pressure. BCB is almost filled into trench except tiny air-polymer mixture at 1 kPa. However, obvious airis still trapped in the trench for 50 kPa. Likewise, as shown in Figure 11(b), the value of square curve (p=1 kPa) is almost equal to one in addition to several tiny valleys (>0.7) existing at bottom and middle of trench, which just corresponds to the tiny air-polymer mixture as previously mentioned. On the circle curve (p=10 kPa), there is a deep valley with value around zero. And on the triangle curve (p=50 kPa), a serious vibration occurs at the middle of trench with value from zero to 0.5, due to initial void being separated during the vacuum treatment process.

So it can be concluded that the pressure has a significant influence on filling performance. The pressure different should be low enough to enable the bubble formation and BCB re-filling. If not, the trapped air cannot be effectively eliminateddespite the further increasing of vacuum treatment duration, which will result in incomplete polymer filling after the pressure pumping up. From the simulation, it is found that 10 kPa is sufficiently low for polymer (BCB 3022-46) filling.

4.3 Effect of viscosity on filling performance

In this case, three types of BCB (listed in Table 2) are used to investigate the effect of viscosity on filling performance. The outlet pressure and the trench width are maintained as 1 kPa and 3 μm, respectively. Because density of the three types has little difference, it can be neglected. Figure 12 shows the contour of volume fraction under different viscosity of polymer at 600 and 650 s. It is apparent that, for the trench filled by polymer 3022-35 (viscosity of 14 cSt), the air has almost been completely eliminated and the polymer has been refilled into the trench without any air. While, for the case of 3022-57 (viscosity of 259 cSt), the air is still within the trench and the polymer has not be completely

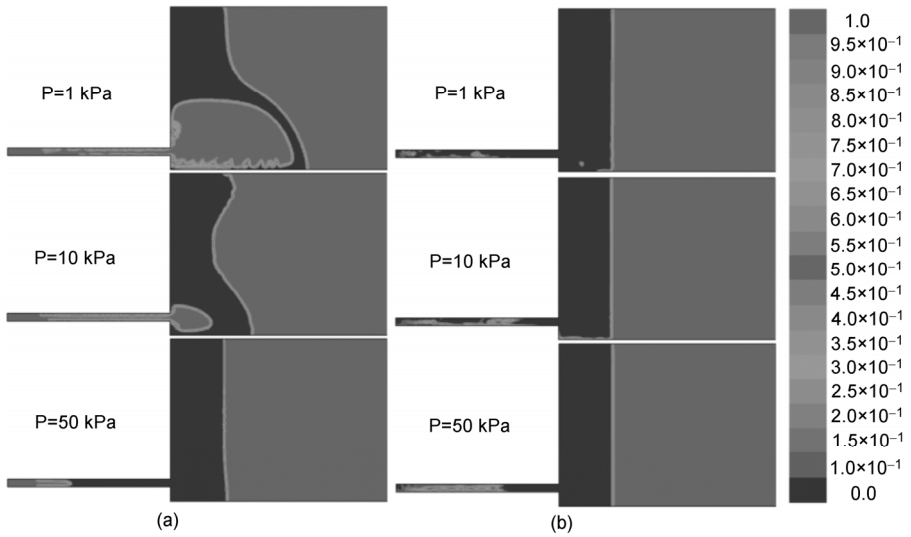

Figure 10 Contour of volume fraction under different outlet pressure, (a) at 0.024s; (b) at 650s.

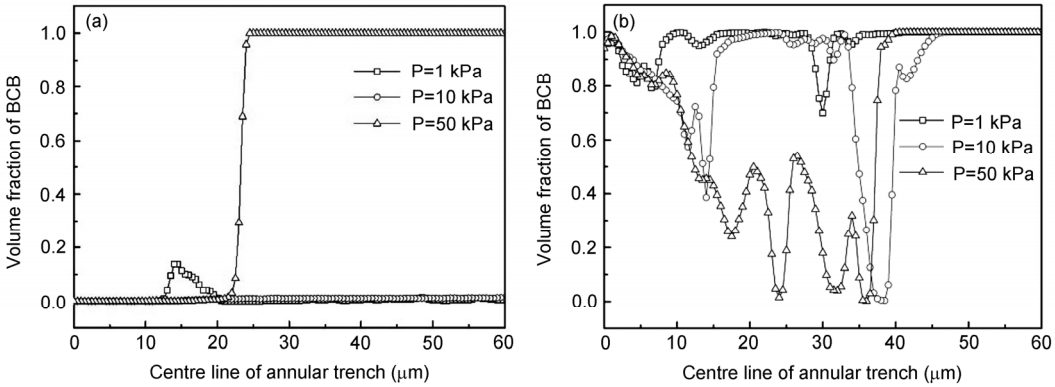

Figure 11 Volume fraction of BCB along the centre line of trench in different pressure outlet, (a) at 0.024 s; (b) at 650 s.

refilled into the trench, an obvious void still exists at the bottom of trench.Compared with the initial void, the void after vacuum treatment has been compressed.

Corresponding to Figure 12, Figure 13 exhibits the detailed distribution of volume fraction of BCB along the centre line of trench under different viscosity at 600 and 650 s. As can be seen from Figure 13(a), in case of 3022-35, BCB almost occupiesthe trench. The opposite case is 3022-57, in other words, air is the dominated one in the trench. After the pressure pumping up at 650 s (Figure 13(b)), the curve of 3022-35 becomes a straight line at the constant of 1.0, indicatingthat there is only BCB in the trench. The triangle

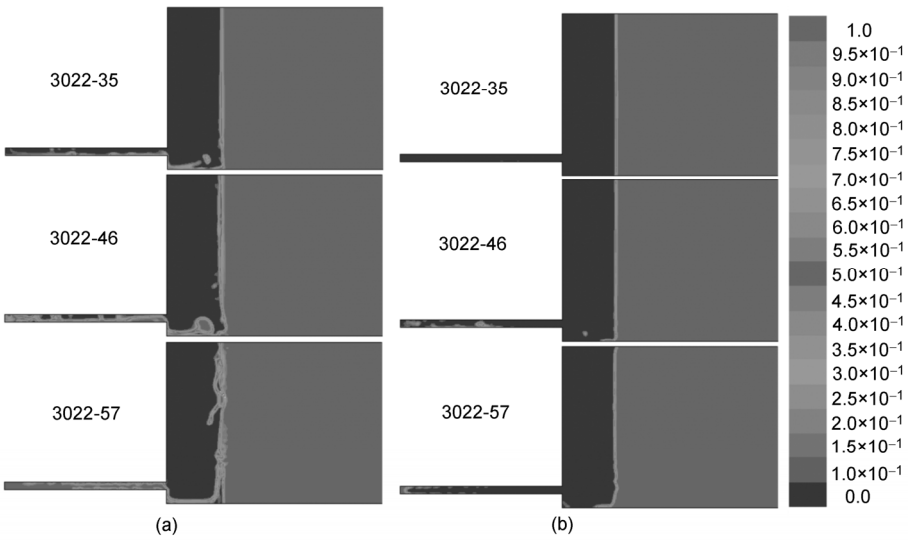

Figure 12 Contour of air volume fraction at different viscosity. (a) At 600 s; (b) at 650 s.

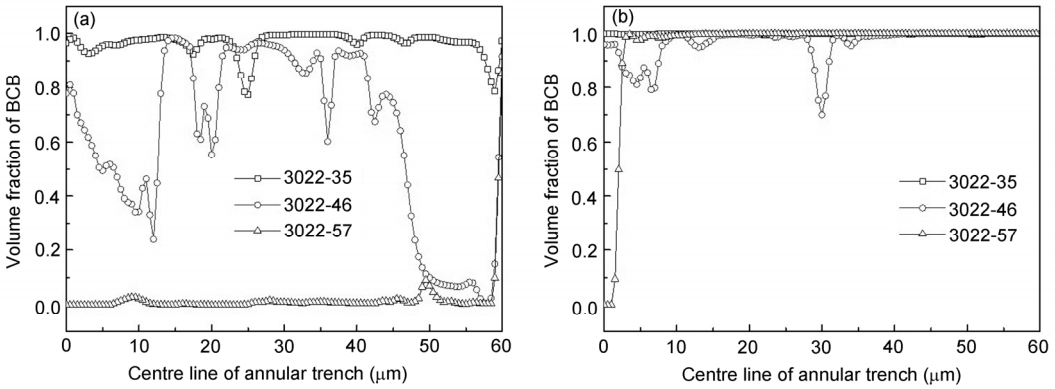

Figure 13 Volume fraction of BCB along the centre line of trench under different viscosity. (a) At 600 s; (b) at 650 s.

curve of 3022-57 shows that there is a large drop, which makes the volume fraction of BCB reach zero at the bottom of trench, that is to say, there is a length of 2 μm void at bottom of trench. The circle curve representing 3022-46 describes the fluctuation along the centre line of trench and the deep valley is the tiny dot mentioned previously.

The simulation results demonstrate that the viscosity of polymer affects the air elimination procedure and higher viscosity needs longer vacuum treatment duration for complete air elimination. Higher viscosity would lead to largerdrag force, which will limit the air elimination velocity. For the case of polymer 3022-57, void-free filling result cannot be expected despite the further increasing of vacuum duration.

4.4 Effect of annular width on filling performance

In this section, the outlet pressure iskept constant as 1kPa,BCB 3022-46 is used,andthe trench width isset as 2, 3 and 5 μm. Figure 14 shows the contour of air volume fraction under different trench width after vacuum treatment for 600 s (Figure 14(a)) and after pressure pumping up at 650 s (Figure 14(b)). It is apparent from Figure 14(a) that the air fills up almost the entire trench with width of 2 μm, while the airalmost escapes from the trench with width of 5 μm. Therefore, as shown in Figure 14(b), after polymer re-filling by pumping up the pressure, obvious void has been formed at the bottom of 2 μm trenchdue to air trapping, and void-free filling results have been achieved for wider trench.

As a supplement to Figure 14, Figure 15 describes the volume fraction of BCB along the centre line of trench under different width at 600 and 650 s. As shown in Figure 15, most part of square curve which represents 2 μm width case isin the zero position, except two peaks at the bottom and middle of trench whose value is no more than 0.75, further confirmingthat the air fills up almost the entire trench. Afterpolymer re-filling, as shown in Figure 15(b), square curvehas a large valley at the bottom of the trench, even most part becomes 1.0. In the case of 3 and 5 μm, they

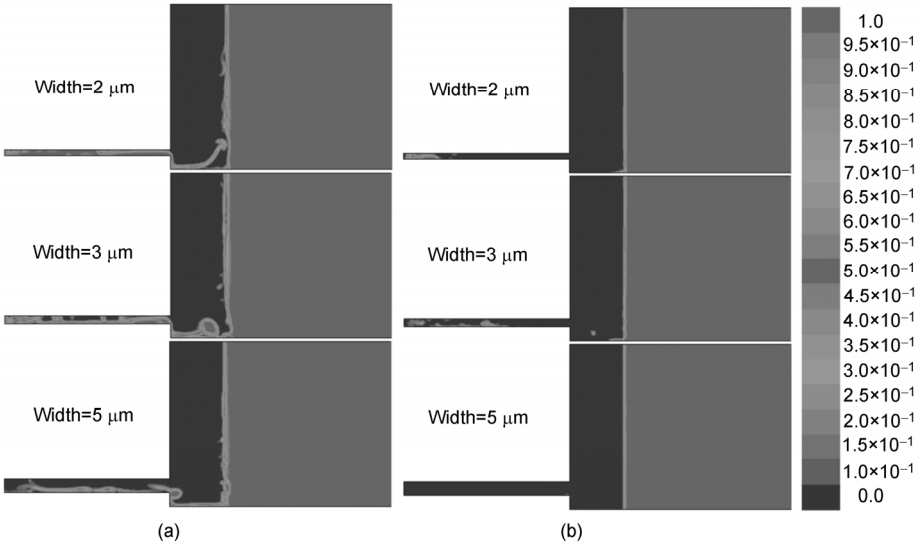

Figure 14 Contour of air volume fraction under different trench width. (a) At 600 s; (b) at 650 s.

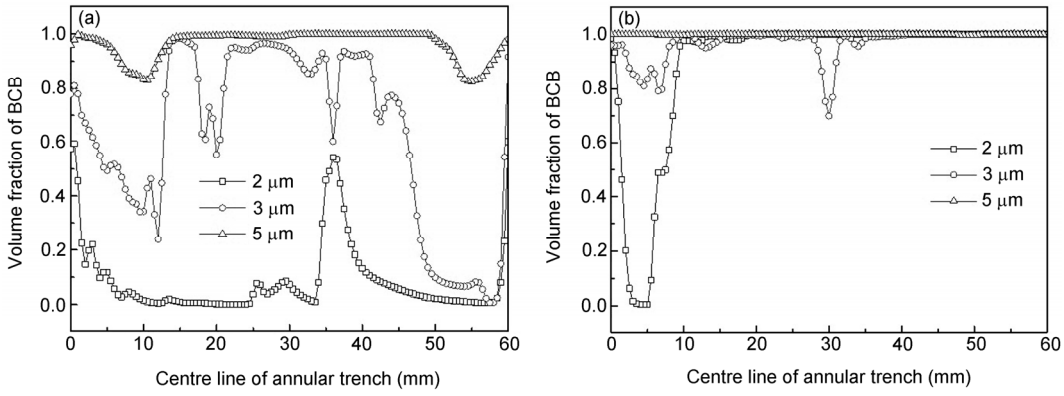

Figure 15 Volume fraction of BCB along the centre line of trench under different trench width. (a) At 600 s; (b) at 650 s.

both have good filling performance.It indicates that with a wider width, there is a better filling,since higher air elimination velocity could be achieved by the reduced drag force with wider trench width.

5 Conclusions

This paper investigated the flow mechanism of the vacuum-ssisted polymer filling process based on experiments and numerical simulation, and studied the effect of vacuum pressure, viscosity of polymer and aspect-ratio of trench on the filling performance. The simulation results indicate that the vacuum-assisted polymer filling process goes through four stages, including bubble formation, bubble burst, air elimination and polymer re-filling. The bubble formation and polymer re-filling proceduresare significantly affected by the pressure, which generates the driving force for void expansion and compression. The outlet pressure should be low enough to enable the bubble formation. The air elimination procedure is time consuming, depending on the poly er viscosity and trench aspect-ratio.The vacuum treatment duration can be reduced by using polymer with lower viscosity and smaller aspect-ratio of trench. For instant, a trench with width of 5 μm and depth of 60 μm can be completely filled with polymer BCB 3022-46 with vacuum treatment at pressure of 1 kPa for 650 s. These results help to better understand the flow mechanism of the vacuum-ssisted polymer filling process, and could help to optimize the process parameters for void-free polymer filling.

1 Lu J Q. 3-D hyperintegration and packaging technologies for micro-nano systems. P IEEE, 2009, 97: 18–30
2 Patti R S. Three-dimensional integrated circuits and the future of system-on-chip designs. P IEEE, 2006, 94: 1214–1224
3 Farooq M G, Iyer S S. 3D integration review. Sci China Inf Sci, 2011, 54: 1012–1025
4 Koester S J, Young A M, Yu R R, et al. Wafer-level 3D integration technology. IBM J Res Dev, 2008, 52: 583–597
5 Sunohara M, Tokunaga T, Kurihara T, et al. Silicon interposer with TSVs (through silicon vias) and fine multilayer wiring. Electronic Components and Technology Conference(ECTC), Lake Buena Vista, Florida, 2008: 847–852
6 Tu K N, Tian T. Metallurgical challenges in microelectronic 3D IC packaging technology for future consumer electronic products. Sci China Tech Sci, 2013, 56: 1740–1748
7 Knickerbocker J U, Andry P S, Dang B, et al. Three-dimensional silicon integration. IBM J Res Dev, 2008, 52: 553–569
8 Topol A W, Tulipe D L, Shi L, et al. Three-dimensional integrated circuits. IBM J Res Dev, 2006, 50: 491–506
9 Ranganathan N, Youhe L, Lo G Q, et al. Influence of Bosch etch process on electrical isolation of TSV structures. IEEE T Compon Pack, 2011, 1: 1497–1507
10 Archard D, Giles K, Price A, et al. Low temperature PECVD of dielectric films for TSV applications.Electronic Components and Technology Conference (ECTC), Las Vegas, Nevada, 2010: 764–768
11 Beica R, Siblerud P, Sharbono C, et al. Advanced metallization for 3D integration. Electronics Packaging Technology Conference (EPTC), Singapore, 2008: 212–218
12 Duval F F, Okoro C, Civale Y, et al. Polymer filling of silicon trenches for 3-D through silicon vias applications. IEEE T Compon Pack, 2011, 1: 825–832
13 Chausse P, Bouchoucha M, Henry D, et al. Polymer filling of medium density through silicon via for 3D-packaging. Electronics Packaging Technology Conference (EPTC), Singapore, 2009: 790–794
14 Coudrain P, Colonna J P, Aumont C, et al. Towards efficient and reliable 300 mm 3D technology for wide I/O interconnects. Electronics Packaging Technology Conference (EPTC), Singapore, 2012: 330–335
15 Duval F, Tezcan D S, Swinnen B, et al. Polymer deep trench filling for Through Silicon Via technology. 13th Meeting for the Symposium on Polymers for Microelectronics, Wilmington, Delaware, 2008
16 Wilke M, Wippermann F, Zoschke K, et al. Prospects and limits in wafer-level-packaging of image sensors. Electronic Components and Technology Conference (ECTC), Lake Buena Vista, Florida, 2011: 1901–1907
17 Truzzi C, Raynal F, Mevellec V. Wet-process deposition of TSV liner and metal films. IEEE 3D System Integration Conference, San Francisco, California, 2009
18 Tezcan D S, Duval F, Philipsen H, et al. Scalable through silicon via with polymer deep trench isolation for 3D wafer level packaging. Electronic Components and Technology Conference (ECTC), San Diego, California, 2009
19 Trichur R K, Fowler M, McCutcheon J W, et al. Filling and Planarizing Deep Trenches with Polymeric Material for Through-Silicon Via Technology. 43rd International Symposium on Microelectronics, Raleigh, North Carolina, 2010: 192–196.
20 Kotb H E M, Isoird K, Morancho F, et al. Filling of very deep, wide trenches by Benzocyclobutene polymer. Microsyst Tech, 2009, 15: 1395–1400
21 Chen Q, Huang C, Wang Z. Benzocyclobutene polymer filling of high aspect-ratio annular trenches for fabrication of through-iliconias (TSVs). Microelectron Reliab, 2012, 52: 2670–2676
22 Chen Q, Huang C, Tan Z, et al. Low capacitance through-silicon-vias with uniform benzocyclobutene insulation layers. IEEE T Compon Pack, 2013, 3: 724–731
23 Batchelor G K. An Introduction to Fluid Dynamics. Cambridge Univ Press, United Kingdom, 2000
24 Brackbill J U, Kothe D B, Zemach C. A continuum method for modeling surface tension. J Comput Phys, 1992, 100: 335–354
25 http://www.dow.com/cyclotene/prod/302235.htm (Processing Procedures for CYCLOTENE 3000 Series Dry Etch Resins) last accessed: June 5, 2013
26 Hirt C W, Nichols B D. Volume of fluid (VOF) method for the dynamics of free boundaries. J Comput Phys, 1981, 39: 201–225
27 Kulkarni A A, Joshi J B. Bubble formation and bubble rise velocity in gas-liquid systems: A review. Ind Eng Chem Res, 2005, 44: 5873–5931